JOURNAL OF Applied Polymer SCIENCE

A Comparative Study of Polyethylene and Polyethylene/C_{60} Nanocomposites Modified with Organic Peroxide

Dong Wan,[1,2] Haiping Xing,[1,2] Feng Liu,[1,2] Lu Wang,[1,2] Yujie Wang,[1,2] Haiying Tan,[1,2] Zhiwei Jiang,[1] Tao Tang[1]

[1]State Key Laboratory of Polymer Physics and Chemistry, Changchun Institute of Applied Chemistry, Chinese Academy of Sciences, Changchun 130022, People's Republic of China

[2]Graduate School of the Chinese Academy of Sciences, Beijing 100039, China

Correspondence to: Z. Jiang (E-mail: jiangzw@ciac.jl.cn) or T. Tang (E-mail: ttang@ciac.jl.cn)

ABSTRACT: Polyethylene (PE)/fullerene C_{60} nanocomposites, and PE samples for comparison in the presence of 0.1 wt % and 0.3 wt % 2, 5-dimethyl-2, 5(tert-butylperoxy) hexane peroxide (DHBP) were prepared by melt mixing. FTIR characterization showed that reactive C_{60} could be grafted onto PE chains via a radical mechanism. As a result, the dispersion state of C_{60} was improved, and the chain extension reaction of PE macroradicals and final topological structures were largely influenced. Linear viscoelastic response of PE and PE/C_{60} nanocomposites containing the same content of peroxide showed much difference. Furthermore, the results of dynamic time sweep tests demonstrated that the addition of C_{60} could accelerate chain extension reaction. The presence of C_{60} could largely improve the thermal stability of PE due to the radical scavenging nature of C_{60}. However, the crystallization behavior, melting behavior and mechanical properties of both PE and PE/C_{60} samples were mainly determined by the content of peroxide. © 2012 Wiley Periodicals, Inc. J. Appl. Polym. Sci. 129: 371–382, 2013

KEYWORDS: polyethylene; fullerene C_{60}; radical reaction; peroxide

Received 18 August 2012; accepted 19 September 2012; published online 16 November 2012
DOI: 10.1002/app.38615

INTRODUCTION

Polyethylene (PE) is the most widely produced and used thermoplastic polymer in the world, with a large versatility of application possibilities. Like polypropylene (PP), PE is easy to undergo the abstraction of hydrogen atoms by alkoxy radicals formed via thermal decomposition of peroxide and produce polymer macroradicals. However, PP macroradicals tend to suffer β-scission reaction and PE macroradicals are prone to undergo radical recombination because of the differences of the chemical structure.[1,2] The formation of PE macroradicals provides us a convenient and useful way to modify PE via melt mixing and broaden its application, such as modification of its polarity by grafting polar monomers,[3,4] adjusting the morphology and properties of PE blending with other polymers,[1,5,6] and production of crosslinked PE in the presence of high content of peroxide to extend its application in hot water pipes, electrical wires and cables, and heat shrinking products.[7,8] It is a question whether PE macroradicals produced during melt mixing can be used to improve the interfacial interaction between PE and nanoparticles. Recently, pentadecane, as a model compound of PE, was used to react with carbon nanotubes (CNTs) in the presence of peroxide.[9,10] The results demonstrated that PE macroradicals could react with the unsaturated bonds located on the surface of CNTs and increase the solubility of CNTs in various solvents. The same group also synthesized the PE-grafted CNTs via a peroxide-initiating radical coupling reaction by using a well-defined TEMPO and thiol end-functionalized PEs in 1, 3-dichlorobenzene.[11]

Fullerene C_{60}, as a special nanoparticle of single molecule, has a high electron affinity and is therefore capable of acting as radical scavengers. The C_{60} has 30 carbon–carbon double bonds that can trap 34 methyl radicals and 15 benzyl radicals at most, thus it is known as a radical sponge.[12] As a reactive nanoparticle, C_{60} has a high addition rate with alkyl radicals with the rate constant in the range of 10^6–10^8 M^{-1} s^{-1}.[13] In our former research,[14] we have demonstrated that the interfacial reaction between C_{60} and PP took place in the presence of peroxide by simple melt mixing. Not only the dispersion state of C_{60} nanoparticles was improved but also the degree of β-scission of PP macroradicals was reduced. Unlike PP macroradicals, PE macroradicals are prone to perform chain extension reactions. In this work, we prepared PE/C_{60} nanocomposites in the presence of relative low content of

Table I. Related Parameters of DHBP at Different Temperatures

T	130°C	150°C	160°C	170°C	180°C
k_d (1/s)	1.20×10^{-4}	1.07×10^{-3}	2.98×10^{-3}	7.89×10^{-3}	2.00×10^{-2}
$t_{1/2}$ (s)	5776.2	647.8	232.6	87.9	34.7

organic peroxide via melt mixing, and studied the influence of reactive C_{60} on the chain structure, rheological, thermal, and mechanical properties of the final PE materials.

EXPERIMENTAL

Materials

A commercial additive-free linear low density polyethylene (LLDPE) powder brand 7042 [(Petrochina Daqing Petrochemical Company, MFR = 2.6 g/10 min (2.16 kg, 190°C)] was used in this study. The C_{60} (purity: 99.9%) was purchased from Yongxin Technology Co., China. The 2, 5-dimethyl-2, 5(tert-butylperoxy) hexane peroxide (DHBP) was obtained from Aldrich. Other reagents were used without further purification. Furthermore, the decomposition rate constant (k_d) and half-life time ($t_{1/2}$) of DHBP at different temperatures were calculated from the following equations and listed in Table I.

$$k_d = A \cdot e^{-E_a/RT} \quad (1)$$

$$t_{1/2} = (\ln 2)/k_d \quad (2)$$

With E_a = 155.49 kJ/mol, $A = 1.68 \times 10^{16}$ 1/s, R = 8.314 J/mol K, which were obtained from the website of AkzoNobel. The residue DHBP at a given time could be acquired from the equation:

$$d[\mathrm{DHBP}]/dt = -k_d[\mathrm{DHBP}] \quad (3)$$

Sample Preparation

All samples without special illustration were prepared via melt mixing at 180°C for 8 min using a Brabender LH60 internal mixer (Shanghai, China) with a rotating speed of 64 rpm. Only 6.77×10^{-3} wt % DHBP was non-decomposed after melt mixing according to eq. (3), and which could be ignored. Torque curves were acquired by Brabender mixing software. Before melt mixing, about 45 g PE power with a designed composition of C_{60} and DHBP was premixed by high speed pulverator for 2 min. After melt mixing, the samples were shaped into 1 mm thick by compressing molding at 170°C. The resultant samples were designated as xCyD. Here C and D denote C_{60} and DHBP, respectively; and x and y denote the weight percentage of C_{60} (×10), and DHBP (×100), respectively. For example, 12C010D means that the sample contains 1.2 wt % C_{60} and 0.1 wt % DHBP. Sample PEB represented pure PE mixing with 1.0 wt % Irganox B215 at the beginning of melt mixing, and other samples were mixed with 1.0 wt % B215 after melt mixing about 7 min.

Characterization

FTIR (Bio-RadFTS-135) was used to characterize PE and modified PE/C_{60} samples, which were pressed into thin films at 150°C. The molecular weight and polydispersity of different PE and PE/C_{60} samples were determined at 150°C by a PL-GPC 220 type high-temperature gel permeation chromatography equipped with differential refractive index. 1, 2, 4-trichlorobenzene was used as solvent at a flow rate of 1.0 mL/min. The calibration was made by the polystyrene standard EasiCal PS-1 (PL). For measuring the content of gel, modified PE and PE/C_{60} samples were first packed with nylon fabric of 500 meshes and extracted in boiling xylene with 0.5 wt % 2, 6-di-tert-butyle-4-methylphenol (BHT) for 24 h. According to the mass change, the gel content of different samples was determined. Morphologies of PE/C_{60} nanocomposites were observed by a transmission electron microscope (TEM, JEL 1011, JEOL, Japan) on microtome sections at 100 kV accelerating voltage. Ultrathin sections were cryogenically cut at a temperature of −80°C using a Leica Ultracut.

Small amplitude dynamic oscillatory shear measurements were carried out on PHYSICA MCR 300 under nitrogen atmosphere. Round samples (25 mm in diameter × 1 mm in thickness) were prepared for frequency scanning at 170°C, with a gap of 0.8 mm and a frequency scope from 0.01 to 100 rad/s. To ensure that the tests were carried out in linear viscoelastic regime, strain sweep was applied for sample PEB, 030D, and 12C30D at a frequency of 1 Hz at 170°C. As shown in Figure 1, the critical strains for linear viscoelastic regime of the samples PEB, 030D, and 12C030D were 40%, 15%, and 11%, respectively. Dynamic time sweep tests were performed by ARES-G2 from TA instruments at different temperatures at a frequency of 1 Hz because the time to get the setting temperature for ARES-G2 was shorter (less than 120 s) than that for PHYSIC MCR 300. The strain for frequency sweep and dynamic time sweep

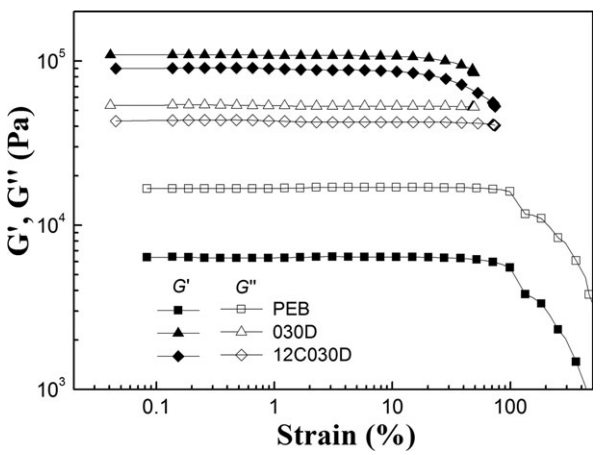

Figure 1. Dynamic strain sweep of samples PEB, 030D, and 12C030D at 170°C.

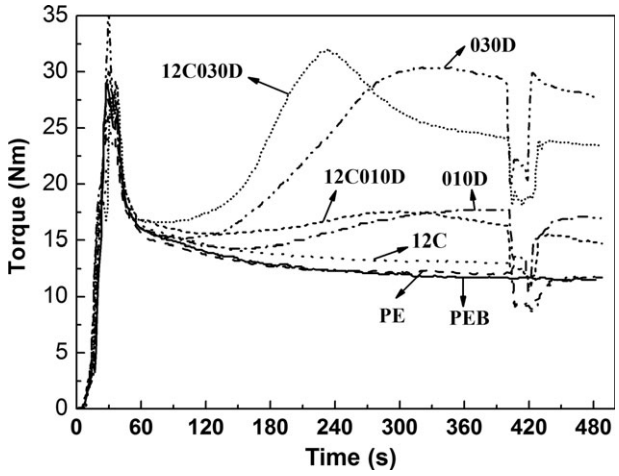

Figure 2. Behavior of the mixing torque for PE and PE/C_{60} samples with or without peroxide at 180°C.

was fixed at 1% in order to make the materials be in the linear viscoelastic regime.

Thermogravimetric analysis (TGA) was done by Thermal Analysis Instrument (SDTQ600, TA Instruments) from 30 to 650°C under air atmosphere with a heating rate of 10°C/min. Melting point and crystallization temperature of the samples were determined by differential scanning calorimetry (DSC) on a Perkin-Elmer DSC-7 instrument, using a heating rate of 10°C/min in the temperature range 20–160°C under nitrogen. The crystallinity was calculated from the ratio of the melting enthalpy of the sample to the melting enthalpy for 100% crystalline PE, with an enthalpy of 293 J/g.[15]

Tensile tests were performed by an Instron Universal Testing Machine (Model 1121) at ambient conditions. The dumbbell shape specimens with gauge dimensions of 20 × 4 × 1 mm^3 were used for tensile test. The crosshead rate was fixed at 20 mm/min and five runs for each sample were measured.

RESULTS AND DISCUSSION

Behavior of Mixing Torque

Both the rate constants of fullerene C_{60} toward alkyl radicals and radical coupling reaction are in the range of 10^6–10^8 M^{-1} s^{-1}.[13,16] Therefore, in principle, adding C_{60} could influence the coupling reaction of PE macroradicals. It is well accepted that the torque value is proportional to the melt viscosity of the polymer. The chain extension reaction will result in the increase of the torque values.[17] As shown in Figure 2, the presence of C_{60} strongly influenced the shape of torque curves in the cases containing peroxide. Without peroxide, a small number of PE macroradicals were formed by thermal initiation. For sample 12C, C_{60} could effectively capture PE macroradicals and form small amounts of long chain branched structure, therefore, the torque values of 12C were larger than those of sample PE after complete fusion of polymer. According to Einstein's viscosity equation,[18] the viscosity of polymer nanocomposites would also increase with the content of nanoparticles. But based on our former research,[19] 1.2 wt % C_{60} had barely influenced the polymer viscosity if no chemical reaction happened. So higher torque values of sample 12C than sample PE should be mainly due to the change of chain structure. In the presence of peroxide, PE underwent chain extension reaction through radical recombination and the torque values increased with the content of peroxide. Further adding C_{60} led to quicker increase of the torque values during 60–240 s, but which showed more obvious decrease later than PE containing the same content of peroxide, because of the changing of the process of radical recombination and chain structure.

Microstructure Characterization of Modified PE/C_{60} Nanocomposites by FTIR and TEM Measurements

FTIR spectroscopy was employed to investigate the chemical reaction between PE chains and C_{60} in the presence of peroxide. At first, sample 12C and 12C030D were purified by dissolving 0.5 g samples in 150 mL xylene at high temperature with 0.5 wt % 2,6-di-tert-butyle-4-methylphenol (BHT) for 2 h and then precipitating by cooling three times to eliminate unreacted C_{60}. Because C_{60} can be dissolved in xylene with the solubility about 5.2 mg/mL at room temperature,[20] only the C_{60} linked to PE chains will precipitate together with PE during cooling. As shown in Figure 3,C_{60} showed two strong characteristic peaks at 526 cm^{-1} and 575 cm^{-1}, but PE had no absorption at the given wavelength range. After purification, the absorption peaks belonging to C_{60} for sample 12C completely disappeared due to little C_{60} linked to PE chains. However, there was an absorption peak at 528 cm^{-1} for sample 12C030D after purification, which demonstrated that a part of C_{60} was covalently grafted onto PE chains through radical reaction. Compared with C_{60}, the shift of 2 cm^{-1} to high wavelength of purified 12C030D could be ascribed to the influence of the bonded bulky PE chain. Additionally, the color of purified 12C030D was brown, and that of purified 12C was almost white, which also confirmed that some C_{60} was covalently grafted onto PE chains for sample 12C030D.

The introduction of chemical linking between polymer matrix and nanoparticles during melt mixing should influence the dispersion state of nanoparticles. The diameter of one C_{60} molecule is 0.71 nm, and different morphologies of crystalline

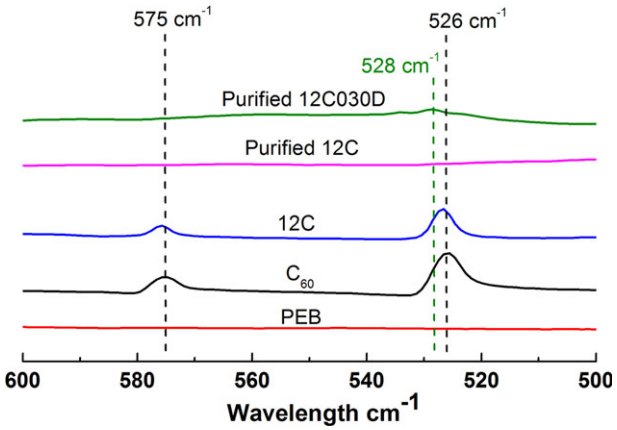

Figure 3. FTIR spectra of C_{60} and different PE/C_{60} samples. [Color figure can be viewed in the online issue, which is available at wileyonlinelibrary.com.]

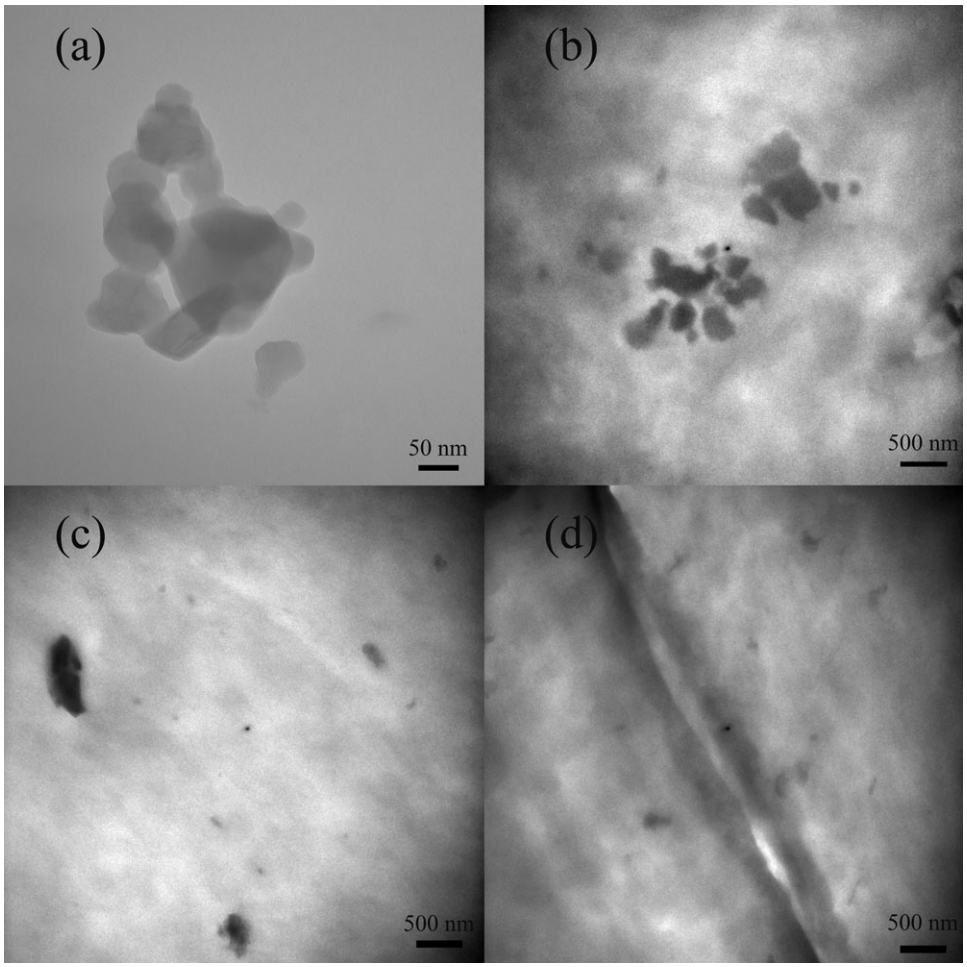

Figure 4. TEM images of (a) C_{60}; (b) 12C; (c) 12C010D; (d) 12C030D.

fullerene solids can be acquired by different precipitation methods.[21,22] Figure 4(a) shows the TEM image of C_{60} from xylene solution, and the size of C_{60} crystals ranged from 30 to 150 nm. The dispersion states of C_{60} in modified PE/C_{60} samples were shown in Figure 4(b–d). Adding an amount of DHBP could improve the dispersion degree of C_{60} in PE matrix. Compared with sample 12C, more small C_{60} clusters were observed for PE/C_{60} nanocomposites containing DHBP. This was ascribed to the improved interfacial interaction between two components and stronger shear force during melt mixing.

Molecular Structure of Modified PE and PE/C_{60} Samples

The possible reactions of PE macroradicals were listed in Scheme 1. Radical coupling reaction of PE macroradicals could lead to chain extension and formation of long chain branched or even crosslinked structure, and disproportion reaction had no influence on the molecular weight. However, β-scission reaction could shorten polymer chain. According to former reports,[1,2] PE macroradicals are prone to undergo radical recombination, whereas PP macroradicals tend to occur with β-scission reaction. The gel content of different PE/C_{60} samples was measured before GPC test. As shown in Table II, gel was only found in the samples 12C010D and 12C030D. The C_{60} can react with more than two free radicals, which can change the topological structure of PE during melt radical reaction.

GPC was used to characterize chain structure of PE/C_{60} samples. As shown in Figure 5(a) and Table II, in the cases without DHBP, PE containing C_{60} (sample 12C) showed higher peak molecular weight (M_p), weight-average molecular weight (M_w), number-average molecular weight (M_n), and broader polydispersity (PDI) than those of sample PE, because of the presence of more fractions of high molecular part. However, in the presence of DHBP, PE samples had different changing trends of molecular weight distributions from PE/C_{60} samples. As shown in Figure 5(b) and Table II, PE samples only containing DHBP showed a gradual increase in the width of the curves and a gradual shift of the M_p and M_w toward higher molecular weights with increasing the content of DHBP. The same phenomenon was also observed in previous reports.[23,24] Nevertheless, the M_p, M_w, and M_n of the soluble part of PE/C_{60} samples decreased with increasing content of DHBP. Especially for sample 12C030D, the M_p and M_w decreased to 38.1 kg/mol and 65.3 kg/mol, respectively. It is because that the probability of forming PE macroradicals is essentially uniform between ethylene units, and polymer chains with higher molecular weight are preferential to form macroradicals and undergo chain extension

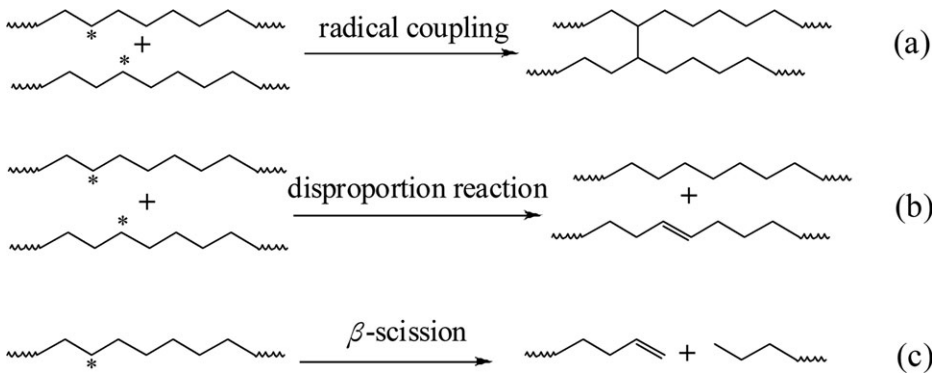

Scheme 1. The possible reactions involved in the life time of PE macroradicals.

reaction.[25] For sample 12C010D and 12C030D, portions of higher molecular weight PE chains in the pristine PE turned into crosslinked structure after modification. Additionally, the β-scission of PE macroradicals is inevitable. Therefore, the soluble parts of 12C010D and 12C030D had much lower M_p, M_w and M_n than sample PEB.

Linear Viscoelastic Properties of Modified PE and PE/C_{60} Samples

Rheology has been proved to be a useful analytical tool to study the molecular architecture.[26–28] Linear viscoelastic properties are very sensitive to the structural change of the materials. The chain scission of polymer will decrease the content of entanglements between polymer chains, and reduce the value of terminal storage modulus (G') and complex viscosity (η^*). However, the presence of long chain branched or crosslinked structure will enhance the chain entanglements, and increase the value of G' and η^* in the low frequency region. Unlike PP macroradicals, the secondary reaction of PE macroradicals was mainly chain extension, rather than chain scission.[1] Because it is not probable for the reactive site to be near the end of the PE chain, the product should own the topological structure of four-arm star if the content of PE macroradical is low, and more complicated network structure in the presence of high content of PE macroradicals. Only a small amount of PE macroradicals were produced uniformly by thermal degradation during the process of melt mixing in the cases without peroxide. However, trace long chain branched structure could influence the relaxation behavior of polymer melts.[29,30] As shown in Figure 6(a), the terminal η^*s of sample PE and 12C were larger than those of sample PEB, because the coupling reaction of PE macroradicals in sample PEB was inhibited because of the presence of 1.0 wt % Irganox B215 at the beginning of melt mixing. Owing to the high addition reaction rate between PE macroradicals and C_{60}, the sample 12C showed a higher η^* in low frequency region than the sample PE. Figure 6(c) shows the storage modulus (G') and loss modulus (G'') of different PE and PE/C_{60} samples without DHBP. Within the terminal zone, linear polymer melts should be fully relaxed and follow the well-known frequency dependence: $G' \sim \omega^2$ and $G'' \sim \omega^1$. The terminal slope of G' and G'' in low frequency region was listed in Table II. Compared with PE, 12C had larger values of G' in low frequency region and lower terminal slope of G' due to the presence of a longer relaxation mechanism.

Figure 6(b) shows the plots of η^* of PE and PE/C_{60} samples in the presence of peroxide. Under this condition, PE macroradicals were mainly produced by alkoxy radicals, and the content of macroradicals was much higher than those produced by thermal degradation. The values of η^* for both PE and PE/C_{60} samples, especially in low frequency region, increased with adding more DHBP. Moreover, the Newtonian plateau in low frequency region of modified PE and PE/C_{60} samples in the presence of peroxide could not be reached because of the increasing content

Table II. The Structural Parameters and Melt Properties of Different PE and PE/C_{60} Samples

Sample	M_p[a] (kg/mol)	M_w (kg/mol)	M_n (kg/mol)	PDI	Gel[b] (wt %)	Slope of G'	Slope of G''	ω_{gel}[c] (rad/s)
PEB	50.5	87.9	22.9	3.84	0	1.42	0.96	-
PE	52.2	90.3	23.5	3.84	0	1.25	0.86	-
12C	56.2	96.3	24.5	3.92	0	1.10	0.78	-
010D	63.5	115.9	26.4	4.39	0	0.52	0.41	-
030D	65.5	155.8	26.4	5.90	0	0.31	0.28	-
12C010D	49.6[d]	95.7[d]	20.4	4.70	6.6	0.48	0.48	2.81
12C030D	38.1[d]	65.3[d]	15.6	4.17	25.0	0.20	0.22	22.23

[a]The peak molecular weight.
[b]The content of gel.
[c]The angular frequency corresponding to the critical gel point.
[d]Soluble component of sample 12C010D and 12C030D.

Applied Polymer SCIENCE

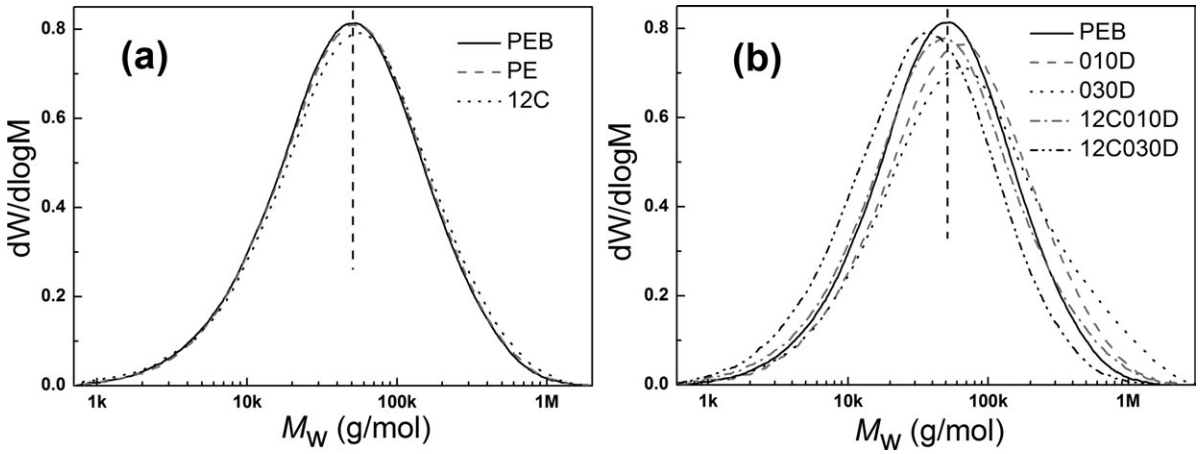

Figure 5. Molecular weight distributions of different PE and PE/C_{60} samples: (a) without DHBP and (b) with DHBP.

of chain entanglements. It was noticeable that sample 12C010D had much lower η^*s than 010D in the given frequency region, but 12C030D had even larger η^*s and more obvious shear thinning phenomenon than 030D in the low frequency region. The similar changing trend was also observed for G' and G'' of different PE and PE/C_{60} samples in the presence of DHBP. As shown in Figure 6(d), the G's and G''s of 12C010D were lower than those of 010D in the testing frequency region; however, 12C030D had even larger terminal G's than 030D in the low frequency region. More importantly, the terminal slope of G' and G'' for both PE and PE/C_{60} in the presence of 0.1 wt % decreased to about 0.5 to perform a gel-like behavior.[31] When

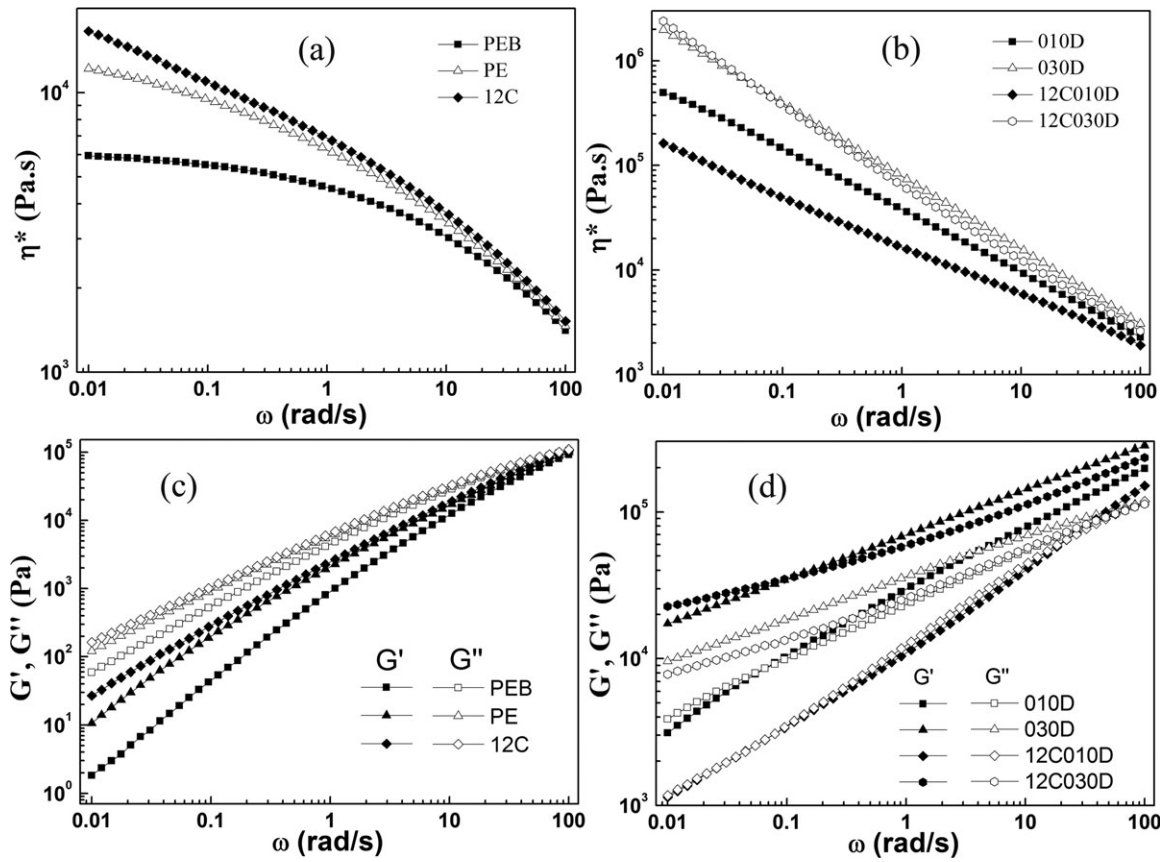

Figure 6. Rheological results of different PE and PE/C_{60} samples: (a) complex viscosity of PE and PE/C_{60} samples without DHBP; (b) complex viscosity of PE and PE/C_{60} samples with DHBP; (c) storage modulus and loss modulus of PE and PE/C_{60} samples without DHBP; and (d) storage modulus and loss modulus of PE and PE/C_{60} samples with DHBP.

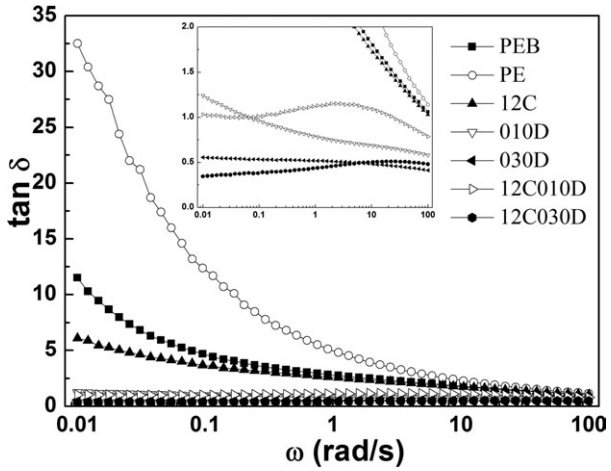

Figure 7. Tan δ versus angular frequency for different PE and PE/C_{60} samples.

adding 0.3 wt % DHBP, the value of G' for 12C030D and 030D was larger than G'' in the given frequency region due to the presence of solid-like behavior.

The tan δ defined by the ratio of G''/G' provides another sensitive way to represent rheological data, especially in the gel-containing system.[32,33] Owing to the connectivity induced by the crosslinked points, the rheological behavior should change from melt-like to solid-like. The so-called "gel point" separates the melt-like behavior from solid-like behavior. According to Fu et al.,[33] at the critical gel point, tan δ is frequency independent, so the critical gel point manifests itself by the appearance of zero-slope "plateau" in the tan δ curve. As shown in Figure 7, compared with sample PEB, all the modified PE and PE/C_{60} samples had much lower tan δ in low frequency region, because of the presence of a longer relaxation mechanism.[34] More importantly, the viscoelastic behavior changing from melt-like to solid-like was only observed for PE samples containing both C_{60} and DHBP due to the formation of crosslinked structure. The angular frequency corresponding to the critical gel point (ω_{gel}, listed in Table II) appeared at a higher frequency for sample 12C030D due to the densification of crosslinked network. It should be noticed that in high frequency region, PE samples had lower tan δ than PE/C_{60} samples containing the same content of DHBP. However, in low frequency region, the reverse phenomenon was found resulting from the influence of C_{60} on the topological structures of PE during melt radical mixing.

The C_{60} is reactive toward free radicals and it can trap more than two PE macroradicals. Comparing with sample 010D, there was about 6.6 wt % gel in sample 12C010D. This portion of gel can be considered as highly branched PE and less entanglements with other polymer chains. Therefore, 12C010D had much lower η^*s and G's than 010D. However, adding 0.3 wt % DHBP, more gel was found in sample 12C030D. Partially continuous networks, rather than separate microgel domains in sample 12C010D, could largely increase the relaxation time of sample 12C030D. As a result, the η^*s and G's of sample 12C030D in low frequency region was even larger than those of 030D.

Thermal Properties of Modified PE and PE/C_{60} Samples

It has been found by Fang's group that C_{60} could enhance thermal properties of PP,[35] HDPE,[36] and HDPE/EVA[37] by a free radical-trapping mechanism. Because polymer materials are usually used under air environment, from a practical application view, it is much more important to evaluate thermal stability of materials under air than under nitrogen. Figure 8 presents the TGA and DTG curves of different PE and PE/C_{60} samples under air environment. The detailed data is listed in Table III. For sample PEB, two-step decomposition processes were observed at around 393°C and 429°C. The same phenomenon was also observed in a previous report.[36] The first step decomposition is the oxidation of PE and the second step may be the decomposition of oxidation products. For PE samples only containing DHBP, the temperature at which 5 wt % mass loss occurred ($T_{5\ wt\ \%}$) decreased with increasing content of DHBP, possibly due to the presence of some shorter PE chains, which was produced by β-scission reaction during melt radical mixing. However, the temperature at which 50 wt % mass loss occurred ($T_{50\ wt\ \%}$) increased with the increasing content of DHBP. This is because chain extension reaction enlarges PE chains.

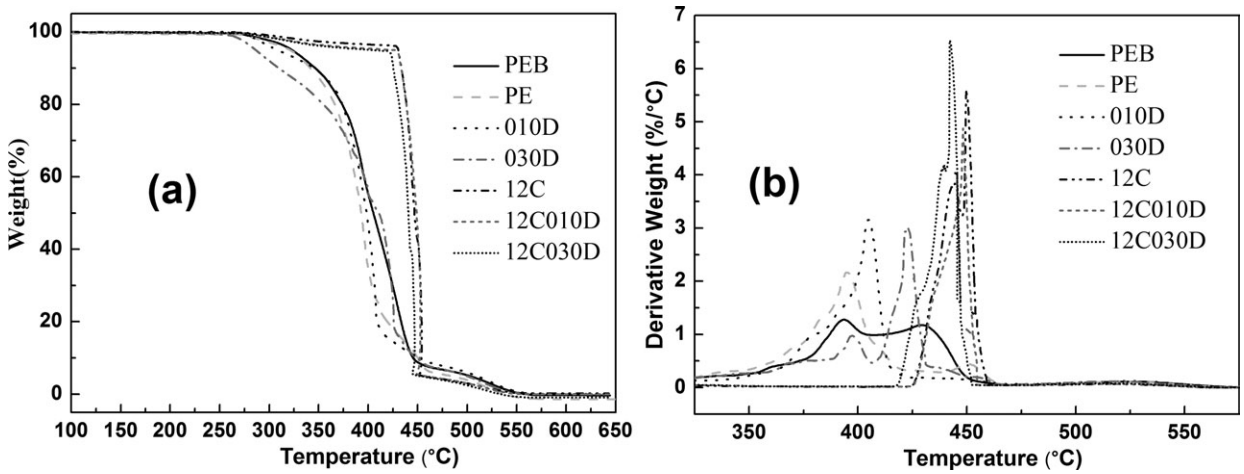

Figure 8. TGA (a) and DTG (b) of different PE and PE/C_{60} samples under air atmosphere.

Table III. Detailed Data of Different PE and PE/C_{60} Samples Obtained from TGA and DSC

Samples	$T_{5\ wt\ \%}$[a] (°C)	$T_{50\ wt\ \%}$[a] (°C)	T_{max}[b] (°C)	T_i (°C)	T_c (°C)	T_m (°C)	χ_c (%)
PEB	323	405	393, 429	109.5	106.1	110.2, 123.2	35.4
PE	321	393	395, 450 (w[c])	110.3	107.0	112.2, 123.5	34.2
010D	308	398	405	109.3	106.5	122.2	34.1
030D	286	411	397 (w[c]), 423	114.0	101.5, 110.1	115.9, 122.0	33.4
12C	430	449	450	109.0	106.0	109.4, 122.2	36.1
12C010D	425	447	448	113.4	100.8, 110.2	114.6, 123.5	34.4
12C030D	407	440	447	113.9	100.5, 111.0	113.6, 123.5	34.4

[a] $T_{5\ wt\ \%}$ and $T_{50\ wt\ \%}$ are the temperatures at which 5 and 50 wt % weight loss occurred, respectively.
[b] T_{max} is the temperature at which the maximum weight loss rate occurred.
[c] "w" means that the peak intensity is weak.

Compared with sample PE, 12C showed noticeably increased $T_{5\ wt\ \%}$, $T_{50\ wt\ \%}$, and T_{max} due to the radical capture nature of C_{60}. Only one T_{max} was observed for all the PE/C_{60} samples, meaning that the presence of C_{60} delayed the oxidation degradation of PE and the first-step T_{max} disappeared. Nevertheless, $T_{5\ wt\ \%}$, $T_{50\ wt\ \%}$, and T_{max} of PE/C_{60} nanocomposites decreased with increasing the content of DHBP, because some C_{60} were consumed by the reaction with PE macroradicals during melt mixing.

The changes in the molecular structure affect the crystallization process, and finally determine the physical and mechanical properties of the semicrystalline materials. The crystallization and melting behavior of different PE and PE/C_{60} samples was compared by means of DSC (Figure 9). The values of initial crystallization temperature (T_i), crystallization peak temperature (T_c), melting temperature (T_m), and crystallinity (χ_c) were summarized in Table III. The T_i, T_c, and χ_c showed almost the same values for sample PEB, PE, and 12C, and we could get a conclusion that very low content of long chain branched PE or the presence of C_{60} did not influence the crystallization of PE. The crystallization process from melt state during DSC measurements was a phase transition process without shear field. According to the rheological results, the η^*s for PE and PE/C_{60} samples in the presence of DHBP in the low frequency region were much higher than those without DHBP due to the increased chain entanglements, implying that zero-shear-rate viscosity was also much higher. The entangled state of polymer chains influences the crystallization process as the rearrangement of chains is necessary to chain folding and perfection. So the presence of long chain branched or crosslinked PE is unfavorable to disentanglement of the chains in polymer melt during crystallization. This was verified by the presence of a new lower crystallization peak in sample 030D, 12C010D, and 030D, and the intensity of lower crystallization peak was even stronger than that of higher crystallization peak for sample 030D and 12C030D [Figure 9(a)]. Though only one T_c was found in sample 010D, the crystallization peak was broader than the samples without peroxide, because of the tougher reorganization of polymer chains. Traditionally, polymer materials crystallize in two steps: nucleation and crystal growth. It is worth to note that the samples 030D, 12C010D, and 12C030D had a much quicker nucleation process than other samples, possibly due to the presence of some shorter PE chains produced by inevitable β-scission reaction. According to the previous reports,[38–40] the nucleation rate increased with decreasing molar mass of PE. The melting temperature and total crystallinity are related to the crystal size and amount of crystals. Almost all the samples, except 010D, had two obvious T_ms [Figure 9(b)]. The

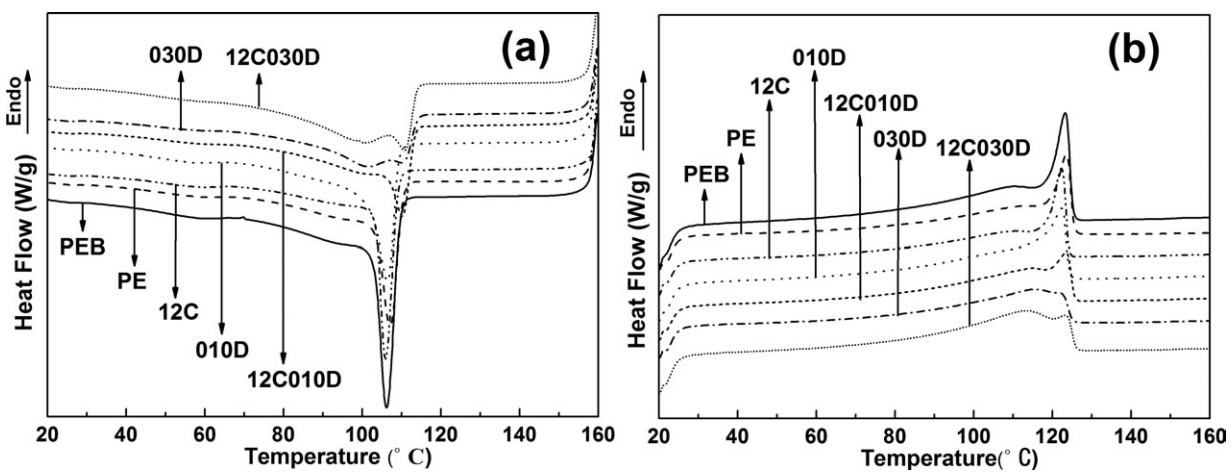

Figure 9. DSC cooling curves (a) and heating curves (b) of different PE and PE/C_{60} samples.

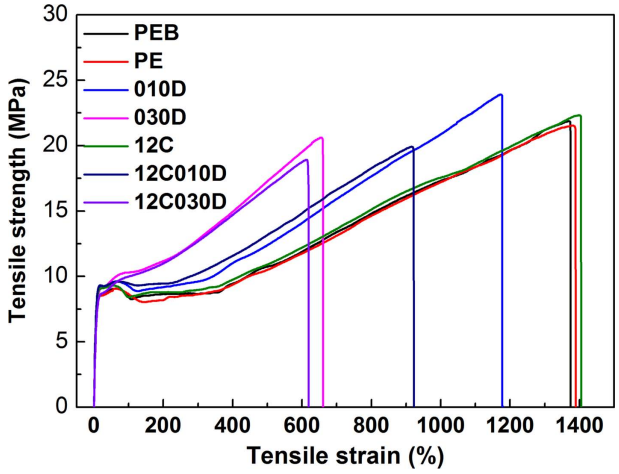

Figure 10. Stress–strain curves of different PE and PE/C_{60} samples at room temperature. [Color figure can be viewed in the online issue, which is available at wileyonlinelibrary.com.]

bimodality observed in the melting process is indicative of the presence of more than one crystalline structure. PE or PE/C_{60} without DHBP had very small endothermic peak at the lower T_m. This phenomenon was widely found in LLDPE.[41–43] The higher T_m corresponds to the molecules with a higher molecular weight, which proportionally possesses a lower number of branching, whereas the valley observed at lower T_m is a result of the crystallization of molecules with a lower molecular weight and a higher content of branching.[43] For samples 030D, 12C010D, and 12C030D, the values of the lower T_m increased compared with those of PE and PE/C_{60} without DHBP, due to different crystalline structures in the presence of highly branched or crosslinked structure. It is worth to note that for the samples 030D and 12C030D, the crystalline enthalpy at lower T_m is even larger than that at higher T_m, implying the existence of the higher content of imperfect crystallite with smaller size.

Mechanical Properties of Modified PE and PE/C_{60} Samples

Many factors can influence the mechanical properties of polymer material, especially in polymer nanocomposites, such as chain structure of polymer, crystallinity, crystal morphology, dispersion state of nanoparticles, interfacial interaction between polymer matrix and nanoparticles. Under stretching at room temperature, PE is ductile and usually yields with necking and drawing followed by strain hardening effect and finally ruptures at relatively long elongation. Comparison of the stress–strain behavior of PE and PE/C_{60} samples with or without peroxide at room temperature is shown in Figure 10 and Table IV. Traditionally, better dispersion of nanoparticles and stronger interfacial interaction between nanoparticles and polymer matrix can maximize the advantage of nanoparticles as effective reinforcing filler in polymer nanocomposites.[44,45] Although the dispersion state of C_{60} and interfacial interaction between PE and C_{60} was improved by *in situ* radical reaction, the tensile properties were mainly influenced by the chain structure and crystal morphology. Tensile strength at yield or 500% increased, but elongation at break decreased with increasing content of DHBP for both PE samples and PE/C_{60} samples, because of the increased branching junctions and chain entanglements, which presented more obvious strain hardening and restriction of chain slippage. Values of Young's modulus are dominated by the amount of hard crystalline regions, unit cells of which are held together by relatively strong forces.[8] However, according to the DSC results, this crystalline structure is being weakened due to the presence of imperfect and smaller size crystal after introducing long chain branched or crosslinked structure. Therefore, Young's modulus of both PE and PE/C_{60} samples decreased with increasing the content of peroxide.

Dynamic Time Sweep Tests of PE and PE/C_{60} Samples Containing DHBP

Traditionally, peroxide crosslinking of PE is performed in two steps. First, a polymer and a certain content of peroxide are mixed at relatively lower temperature, and the premixture is subsequently treated at higher temperature to perform chain extension reactions.[46] Here, we used dynamic time sweep tests to study the *in situ* chain extension reactions of PE and PE/C_{60} in the presence of 0.3 wt % DHBP at different temperatures. The premixtures were processed at 130°C for 200 s and compressed into 1 mm round discs with the diameter of 25 mm at 130°C. The PE and PE/C_{60} containing 0.3 wt % DHBP mixed at 130°C were nominated as L030D and L12C030D, respectively, distinguishing from the samples mixed at 180°C. As shown in Table I, the half-life time of DHBP at 130°C is long, and the decomposition of DHBP during premixing at this temperature can be neglected. This was also confirmed by torque curves at 130°C (Figure 11). The torque values of both L030D and

Table IV. Mechanical Properties of Different PE and PE/C_{60} Samples

Sample	Tensile strength at yield (MPa)	Tensile strength at 500% (MPa)	Tensile strength at break (MPa)	Young's modulus (MPa)	Elongation at break (%)
PEB	9.2 ± 0.1	10.8 ± 0.1	21.3 ± 0.2	189 ± 9	1342 ± 10
PE	9.1 ± 0.1	10.6 ± 0.1	21.4 ± 0.1	184 ± 14	1356 ± 31
010D	9.5 ± 0.1	12.4 ± 0.1	24.6 ± 0.2	183 ± 10	1199 ± 34
030D	10.1 ± 0.1	17.2 ± 0.1	20.2 ± 0.5	149 ± 5	647 ± 25
12C	9.3 ± 0.1	10.9 ± 0.1	21.8 ± 0.2	188 ± 12	1325 ± 30
12C010D	9.5 ± 0.1	13.1 ± 0.1	19.8 ± 0.1	170 ± 14	918 ± 30
12C030D	9.9 ± 0.1	16.8 ± 0.1	19.2 ± 0.2	134 ± 4	587 ± 25

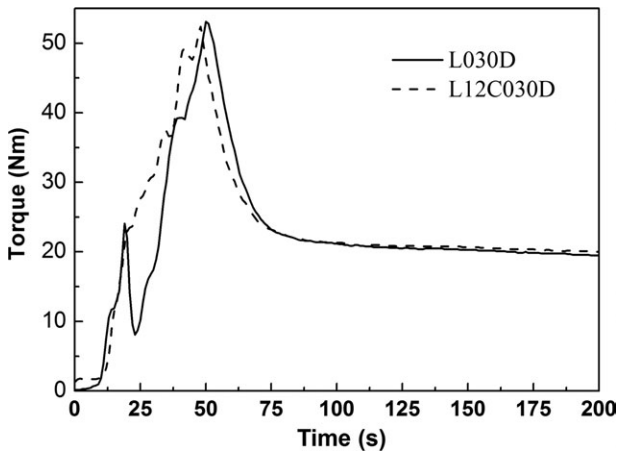

Figure 11. Torque curves of PE and PE/C_{60} in the presence of 0.3 wt % DHBP at 130°C.

L12C030D almost kept constant after complete fusion of PE and were much different with the samples mixed at 180°C (Figure 2).

The results of dynamic time sweep tests at different temperatures are shown in Figure 12. Molecular chain mobility is strongly affected when chain extension reactions occur. Both G' and G'' increased with time at first and approached equilibrium at a longer time, but G'' was not as sensitive as G' to the presence of branched structures. At a particular point, G' and G'' intersected with each other, except sample L12C030D at 170°C. The crossover of G' and G'' denotes the transition from viscous dominant behavior ($G'' > G'$) to elastic dominant behavior ($G' > G''$), which is caused by the sufficient entanglements of polymer chains.[47] The time and G' at crossover ($t_{crossover}$ and $G'_{crossover}$), and G' and G'' at equilibrium (G'_{eq} and G''_{eq}) were summarized in Table V. As expected, $t_{crossover}$ for both L030D and L12C030D decreased with increasing temperature as peroxide decomposed faster at higher temperatures. The $t_{crossover}$ of sample L12C030D was much shorter than that of sample L030D at the same temperature, because of much quicker chain extension reaction in the presence of C_{60}. It was worth to note that $G'_{crossover}$ for both L030D and L12C030D were close to 4.4×10^4 Pa at 150°C and 160°C, which might imply that the content of entanglements between PE chains was nearly the same at the intersection of G' and G''. However, the value of $G'_{crossover}$ at 170°C showed much difference, possibly due to the consumption of some DHBP before starting dynamic time sweep tests, if we considered the $t_{1/2}$ of DHBP at 170°C only 87.9 s. The decomposed weight percentage of DHBP at $t_{crossover}$ (D_{DHBP}) was calculated according to eq. (3) and listed in Table V. The D_{DHBP} for L030D at 150°C and 160°C was the same, meaning that apparent efficiency of free radical to create an entangled network did not depend on the decomposition temperature of DHBP but only of the decomposed DHBP. However, D_{DHBP} for L12C030D at 160°C was much lower than that at 150°C, because of the change of the process of chain extension reaction by C_{60}.

Both G'_{eq} and G''_{eq} for L030D and L12C030D at 160°C were higher than those at 150°C or 170°C, implying that moderate decomposition rate of DHBP was better to increase elastic behavior of PE. This effect was more obvious for L12C030D. G'_{eq} at 160°C for L12C030D was almost 1.35 times higher than that at 150°C and 1.61 times higher than that at 170°C, whereas G'_{eq} at 160°C for L030D was only 1.12 and 1.30 times higher than those at 150 and 170°C, respectively. It was worth to note that though G'_{eq} for L12C030D was higher than that of L030D at a given temperature, G''_{eq} for L12C030D was lower than that of L030D. The G' is taken as a measure of the energy stored in the materials and recovered from it per cycle, and is dependent on what rearrangements can take place within the period of oscillation, which is used to estimate the elastic behaviors of the materials. In contrast, G'' measures the energy dissipated or lost per cycle of sinusoidal deformation, and it is characteristic of the viscous behaviors.[48] We could get the conclusion that the chain structures of PE samples containing both C_{60} and DHBP was not as uniform as PE samples only containing DHBP. Because higher content of large PE network in L12C030D was formed after high temperature treatment, which could store more energy, whereas higher content of small PE chains also existed in L12C030D that could dissipate more energy.

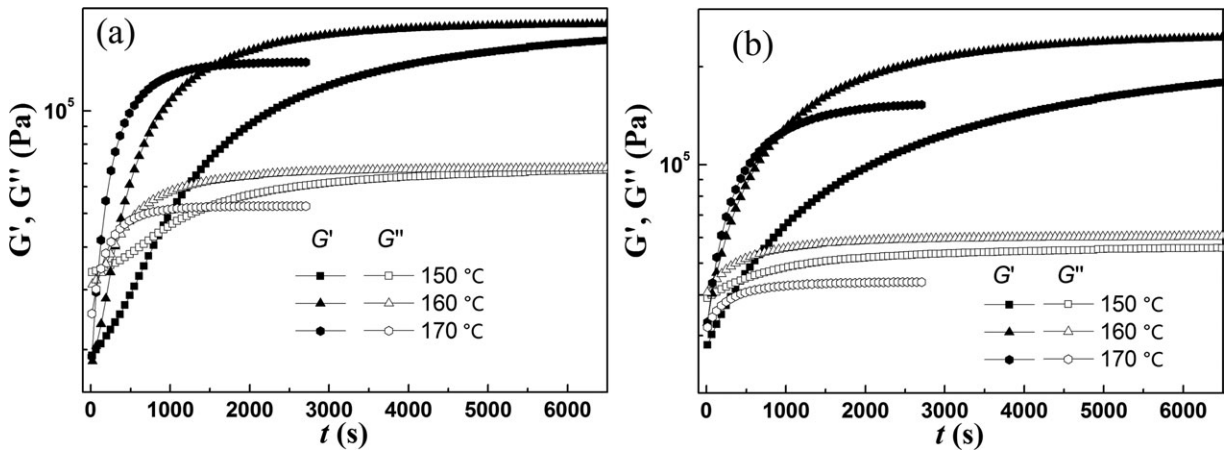

Figure 12. Dynamic time sweep tests of (a) L030D and (b) L12C030D at different temperatures.

Table V. Related Parameters Obtained from Dynamic Time Sweep Tests

	L030D					L12C30D				
T (°C)	$t_{crossover}$ (s)	$G'_{crossover}$ (Pa)	D_{DHBP} (%)	G'_{eq} (Pa)	G''_{eq} (Pa)	$t_{crossover}$ (s)	$G'_{crossover}$ (Pa)	D_{DHBP} (%)	G'_{eq} (Pa)	G''_{eq} (Pa)
150	877.6	44300	60.9	161000	67100	436.0	44300	37.3	181000	55800
160	314.9	40900	60.9	181000	68100	105.2	44100	26.9	246000	60300
170	74.1	30500	44.3	139000	52600	-	-	-	153000	43800

CONCLUSIONS

In situ interfacial reaction between reactive C_{60} and PE in the presence of organic peroxide occurred via a free radical mechanism during melt mixing. The dispersion state of C_{60} was improved because of the chemical linking between two components and increased shear force. The C_{60} strongly influenced the process of chain extension reactions of PE macroradicals and changed the chain structure of PE. The PE/C_{60} nanocomposites had a certain content of gel even at 0.1 wt % DHBP, this was different from PE samples only containing peroxide. It is worth to note that PE/C_{60} nanocomposites containing peroxide had much quicker chain extension reactions and larger values of G' at equilibrium at different temperatures than PE samples containing the same content of peroxide. Owing to the radical scavenging nature of C_{60}, PE/C_{60} nanocomposites had largely improved thermal stability comparing to PE samples. Although the interfacial interaction between PE and C_{60} and the dispersion state of C_{60} were improved in the presence of peroxide, the mechanical properties of PE/C_{60} nanocomposites were more strongly influenced by the changing of chain structures and crystalline morphology, if we comparatively studied these of the PE samples.

ACKNOWLEDGMENTS

This work is financially supported by the National Natural Science Foundation of China for the Projects (51073149 and 50873099) and the Fund for Creative Research Groups (No. 50921062).

REFERENCES

1. Braun, D.; Richter, S.; Hellmann, G. P.; Rätzsch, M. *J. Appl. Polym. Sci.* **1998**, *68*, 2019.
2. Zhou, W.; Zhu, S. *Macromolecules* **1998**, *31*, 4335.
3. Samay, G.; Nagy, T.; White, J. L. *J. Appl. Polym. Sci.* **1995**, *56*, 1423.
4. Gaylord, N. G.; Mehta, R. *J. Polym. Sci. Part A: Polym. Chem.* **1988**, *26*, 1189.
5. Sirin, K.; Balcan, M. *Polym. Adv. Technol.* **2010**, *21*, 250.
6. An, Y. J.; Zhang, Z. J.; Wang, Y. H.; Qiu, J.; Tang, T. J. *J. Appl. Polym. Sci.* **2010**, *116*, 1739.
7. Han, S. O.; Lee, D. W.; Han, O. H. *Polym. Degrad. Stab.* **1999**, *63*, 237.
8. Khonakdar, H. A.; Morshedian, J.; Wagenknecht, U.; Jafari, S. H. *Polymer* **2003**, *44*, 4301.
9. Akbar, S.; Beyou, E.; Chaumont, P.; Melis, F. *Macromol. Chem. Phys.* **2010**, *211*, 2396.
10. Akbar, S.; Beyou, E.; Cassagnau, P.; Chaumont, P.; Farzi, G. *Polymer* **2009**, *50*, 2535.
11. Akbar, S.; Beyou, E.; Chaumont, P.; Mazzolini, J.; Espinosa, E.; D'Agosto, F.; Boisson, C. *J. Polym. Sci. Part A: Polym. Chem.* **2011**, *49*, 957.
12. Krusic, P. J.; Wasserman, E.; Keizer, P. N.; Morton, J. R.; Preston, K. F. *Science* **1991**, *254*, 1183.
13. Zeynalov, E. B.; Allen, N. S.; Salmanova, N. I. *Polym. Degrad. Stab.* **2009**, *94*, 1183.
14. Wan, D.; Zhang, Z.; Wang, Y.; Xing, H.; Jiang, Z.; Tang, T. *Soft Matter* **2011**, *7*, 5290.
15. Jong-Il, W. *Polym. Degrad. Stabil.* **2010**, *95*, 14.
16. Odian, G. Principles of Polymerization. John Wiley & Sons Inc.: New Jersey, **2004**, p 204.
17. Romani, F.; Corrieri, R.; Braga, V.; Ciardelli, F. *Polymer* **2002**, *43*, 1115.
18. Einstein A. *Ann. Phys. Berlin.* **1906**, *19*, 371.
19. Wan, D.; Wang, Y. J.; Wen, X.; Qiu, J.; Jiang, Z. W.; Tan, H. Y.; Tang, T. *Polym. Eng. Sci* **2012**, *52*, 1457.
20. Ruoff, R. S.; Tse, D. S.; Malhotra, R.; Lorents, D. C. *J. Phys. Chem.* **1993**, *97*, 3379.
21. Minato, J.; Miyazawa, K. *Carbon* **2005**, *43*, 2837.
22. Miyazawa, K.; Hotta, K. *J. Cryst. Growth.* **2010**, *312*, 2764.
23. Perez, C. J.; Cassano, G. A.; Valles, E. M.; Failla, M. D.; Quinzani, L. M. *Polymer* **2002**, *43*, 2711.
24. Lem, K. W.; Han, C. D. *J. Appl. Polym. Sci.* **1982**, *27*, 1367.
25. Parent, J. S.; Sengupta, S. S.; Kaufman, M.; Chaudhary, B. I. *Polymer* **2008**, *49*, 3884.
26. Munstedt, H. *Soft Matter* **2011**, *7*, 2273.
27. Stefan Trinkle; Friedrich, C. *Rheol. Acta.* **2001**, *40*, 322.
28. Trinkle, S.; Walter, P.; Friedrich, C. *Rheol. Acta.* **2002**, *41*, 103.
29. Keβner, U.; Munstedt, H. *Polymer* **2010**, *51*, 507.
30. McCallum, T. J.; Kontopoulou, M.; Park, C. B.; Muliawan, E. B.; Hatzikiriakos, S. G. *Polym. Eng. Sci.* **2007**, *47*, 1133.
31. Hayashida, K.; Tanaka, H.; Watanabe, O. *Polym. Int.* **2011**, *60*, 1194.
32. Garcia-Franco, C. A.; Srinivas, S.; Lohse, D. J.; Brant, P. *Macromolecules* **2001**, *34*, 3115.
33. Fu, B. X.; Gelfer, M. Y.; Hsiao, B. S.; Phillips, S.; Viers, B.; Blanski, R.; Ruth, P. *Polymer* **2003**, *44*, 1499.
34. Graebling, D. *Macromolecules* **2002**, *35*, 4602.

35. Fang, Z. P.; Song, P. A.; Tong, L. F.; Guo, Z. H. *Thermochim. Acta.* **2008**, *473*, 106.

36. Zhao, L. P.; Song, P. A.; Cao, Z. H.; Fang, Z. P.; Guo, Z. H. *J. Nanomater.*, **2012**.

37. Liu, H.; Song, P. A.; Fang, Z. P.; Shen, L.; Peng, M. *Thermochim. Acta.* **2010**, *506*, 98.

38. Krumme, A.; Lehtinen, A.; Viikna, A. *Eur. Polym. J.* **2004**, *40*, 371.

39. Krumme, A.; Lehtinen, A.; Viikna, A. *Eur. Polym. J.* **2004**, *40*, 359.

40. Xue, Y. N.; Wang, Y. H.; Liu, F.; Li, Y.; Tang, T. *Chem. J. Chin. Univ.-Chin.* **2009**, 30, 1870.

41. Watanabe, S.; Sano, N.; Noda, I.; Ozaki, Y. *J. Phys. Chem. B* **2009**, *113*, 3385.

42. Perera, R.; Albano, C.; Sanchez, Y.; Karam, A.; Silva, P.; Pastor, J. M. *J. Appl. Polym. Sci.* **2012**, *124*, 1106.

43. Kim, M.-H.; Phillips, P. J. *J. Appl. Polym. Sci.* **1998**, 70, **1893**.

44. Hwang, G. L.; Shieh, Y. T.; Hwang, K. C. *Adv. Funct. Mater.* **2004**, *14*, 487.

45. Coleman, J. N.; Khan, U.; Gun'ko, Y. K. *Adv. Mater.* **2006**, *18*, 689.

46. Smedberg, A.; Hjertberg, T.; Gustafsson, B. *Polymer* **1997**, *38*, 4127.

47. Liu, M. G.; Zhou, C. X.; Yu, W. *Polym. Eng. Sci.* **2005**, *45*, 560.

48. Wei, S. S.; Zhang, Y.; Xu, J. R. *J. Polym. Res.* **2011**, *18*, 125.